Supporting Information

Correlating Structure, Conductance and Mechanics of Silver Atomic-Scale Contacts

Sriharsha V. Aradhya [1,†], Michael Frei [1,†], András Halbritter [2] and Latha Venkataraman [1,*]

1. Department of Applied Physics and Applied Mathematics, Columbia University, New York, NY, USA

2. Department of Physics, Budapest University of Technology and Economics and Condensed Matter Research Group of the Hungarian Academy of Sciences, Hungary

Contents

I. Defining conductance ranges: 2

II. Data analysis - conductance: 2

III. Data analysis - force: 4

IV. Conductance cross-correlation analysis: 5

V. References: 6

I. Defining conductance ranges:

Figure S1 shows the logarithmically binned one-dimensional conductance histogram of 10,000 Ag traces measured with the STM-BJ setup, which visualizes the same data represented in Figure 2a in the main text. In the logarithmically binned histogram the peaks in the conductance data, as well as their minima, appear more clearly. This allows us to define the conductance ranges for the Ag-SAC (0.7 G_0 – 1.0 G_0), AgO-S (0.25 G_0 – 0.55 G_0) and AgO-P (1.0 G_0 – 1.4 G_0), as highlighted by the shaded regions in Figure S1.

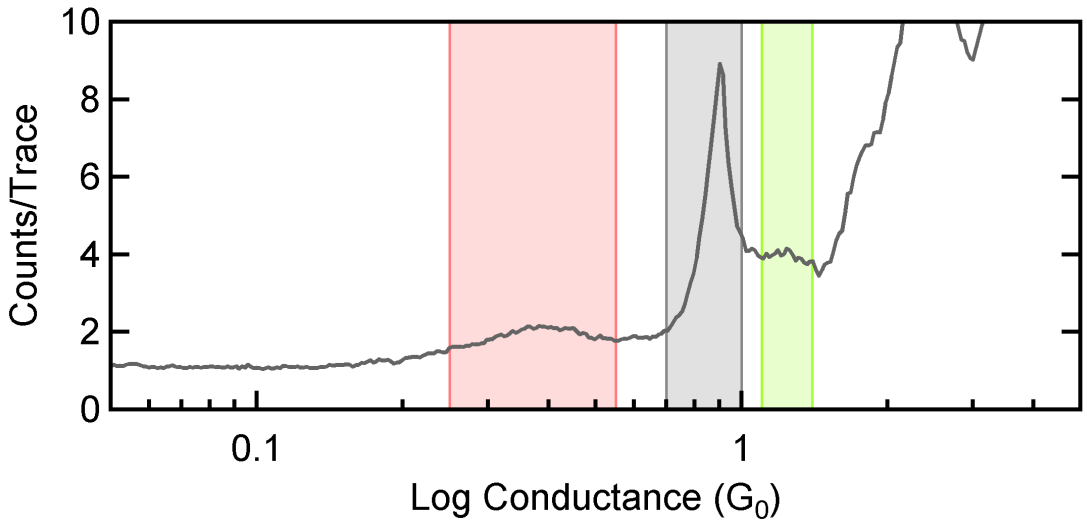

Figure S1. Logarithmically binned one-dimensional histogram (10,000 traces, 167 bins per decade). Ag-SAC (grey), AgO-S (red) and AgO-P (green) conductance ranges are highlighted.

II. Data analysis - conductance:

Figure S2 shows additional sample traces for each of the cases discussed in the main text. Figure S2a represents an Ag-SAC junction that ruptures after the 1 G_0 conductance plateau. Conductance features at 1.8 G_0 and 2.5 G_0 are also observed before the 1 G_0 plateau. Figure S2b,c represent AgO-P (with a plateau at ~1.3 G_0) junctions. In addition to the AgO-P conductance plateau, an additional feature at ~0.3 G_0 that can be ascribed to an evolution into

AgO-S structure is also observed in Figure S2b (AgO-P to AgO-S scenario). However, in Figure S2c the AgO-P junction is completely ruptured upon elongation (AgO-P to rupture). Therefore, traces such as those in Figure S2b and Figure S2c are included in AgO-P, but only traces such as figure S2c are included in AgO-P to rupture scenario. Finally, Figure S2d shows a representative AgO-S junction, with a plateau at ~0.3 G_0, where we also note the absence of any conductance feature at 1 G_0 corresponding to the Ag-SAC, which reflects the anti-correlation between 1 G_0 and 0.4 G_0 features observed in the cross-correlation analysis presented in the main text (Fig. 2c).

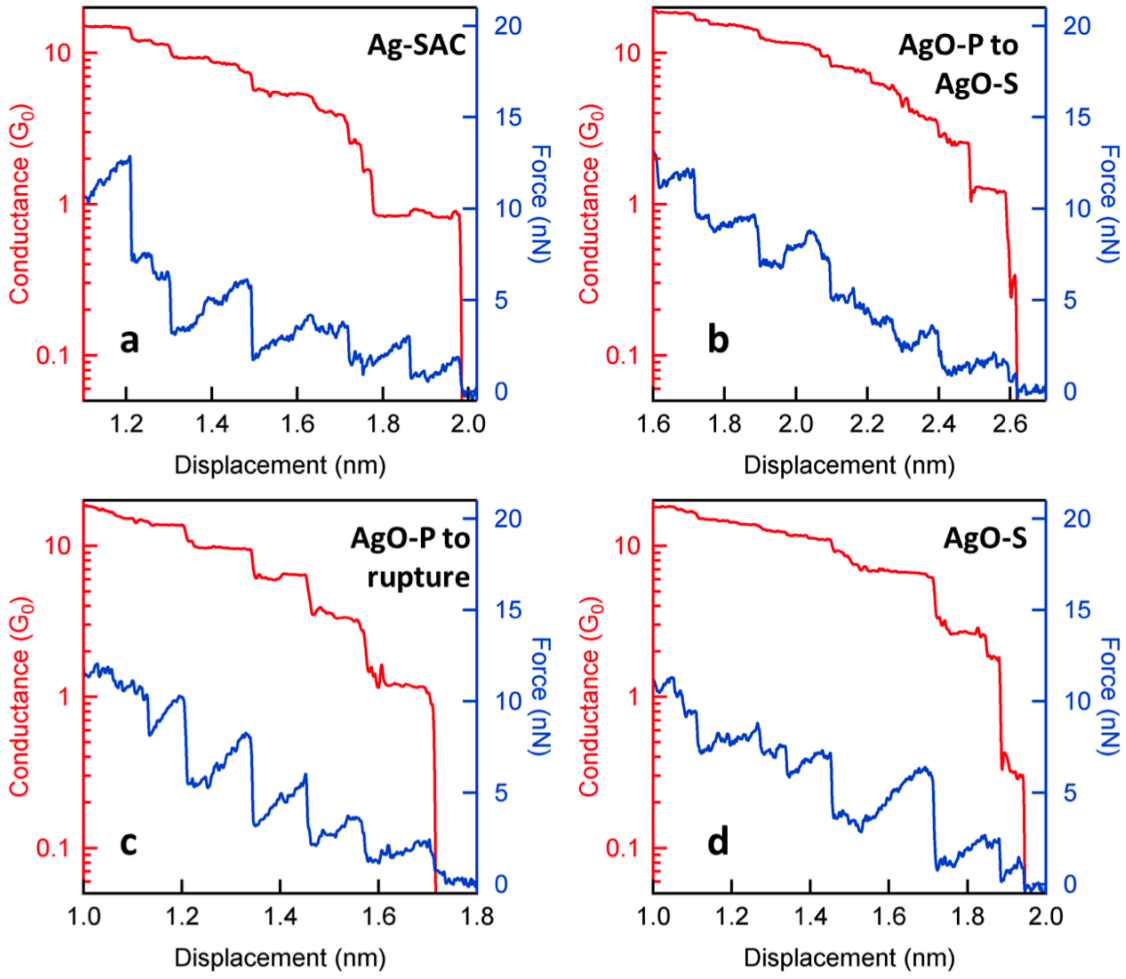

Figure S2. Sample traces showing the simultaneously measured conductance (red, left axis) and force (blue, right axis): Ag-SAC (a), AgO-P to AgO-S (b), AgO-P to rupture (c) and AgO-S (d).

III. Data analysis - force:

In Figure S2a, an additional force saw-tooth can be seen over the $1G_0$ conductance plateau, in addition to the final saw-tooth feature of interest. This is due to atomic-scale mechanical rearrangements, which nonetheless cannot be identified in the conductance data. In order to obtain a reliable stiffness from the force data, these additional rearrangement events must be avoided in order to define the final loading and rupture event for the junction of interest.

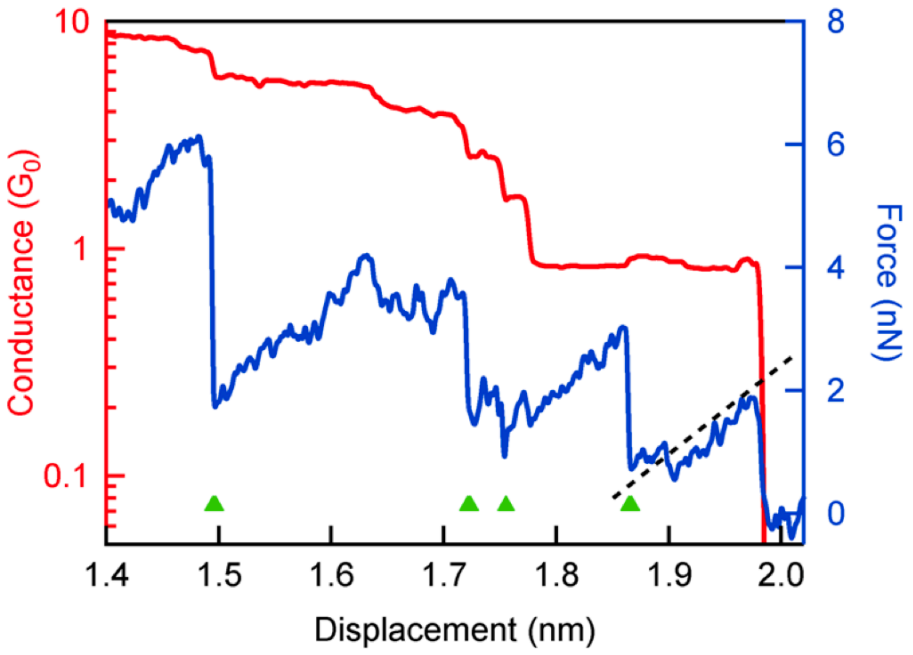

Figure S3. A zoomed-in view of the conductance (red, left axis) and force (blue, right axis) for Ag-SAC. An automated algorithm identifies significant force events prior to junction rupture (green markers). Stiffness can therefore be reliably defined over the final loading event before junction rupture by a linear fit to the force data (dashed line).

We use a previously described automated algorithm[1] to identify significant force events, i.e., *sharp and large* fluctuations beyond the experimental noise level. We begin by identifying the location of junction rupture through the conductance data. As an example, Figure S3 shows a

zoomed-in view near the Ag-SAC $1G_0$ region of Figure S2a. The junction rupture from the $1G_0$ plateau can be clearly seen at 1.98 nm along the displacement axis. We then separately analyze low- and high-pass filtered force data and identify every force fluctuation greater than 0.25 nN (which is ~1.5× the standard deviation of our instrumental noise).

In Figure S3, these algorithmically identified force fluctuation events are shown by the green markers. The force data between the last identified force event and the junction rupture is fitted with a linear fit (dashed line in Figure S3), and the slope of this line represents the effective stiffness (K_{eff}) of the junction (K_{junc}) in series with the cantilever (K_{cant}). To extract the junction stiffness of the junction alone we compute $K_{junc} = (K_{eff} \times K_{cant}) / (K_{cant} - K_{eff})$, with K_{cant} = 50 N/m obtained from the experimental calibration of the AFM cantilever[2].

IV. Conductance cross-correlation analysis:

We follow the methods of Halbritter *et al.*[3, 4] to perform the conductance cross-correlation analysis. We create the 2D cross-correlation histogram shown in Figure 2b within the main text with bins of size 0.01 G_0 spanning 0 to 4 G_0. The value of each bin in the 2D conductance is:

$$C_{i,j} = \frac{\left\langle \delta N_i(r) * \delta N_j(r) \right\rangle_r}{\sqrt{\left\langle \left[\delta N_i(r)\right]^2 \right\rangle_r \left\langle \left[\delta N_j(r)\right]^2 \right\rangle_r}} \quad \ldots (1)$$

where the subscripts *i, j* identify the bin in the horizontal and vertical axes, while *r* is an index representing each trace included in the calculation. The $\langle ... \rangle$ represent an average over all traces *r* and $\delta N \equiv N_i(r) - \langle N_i(r) \rangle_r$.

V. References:

(1) Aradhya, S. V.; Frei, M.; Hybertsen, M. S.; Venkataraman, L. Van Der Waals Interactions at Metal/Organic Interfaces at the Single-Molecule Level. *Nat. Mater.* **2012**, *11*, 872-876.

(2) Hutter, J. L.; Bechhoefer, J. Calibration of Atomic-Force Microscope Tips. *Rev. Sci. Instrum.* **1993**, *64*, 1868-1873.

(3) Halbritter, A.; Makk, P.; Mackowiak, S.; Csonka, S.; Wawrzyniak, M.; Martinek, J. Regular Atomic Narrowing of Ni, Fe, and V Nanowires Resolved by Two-Dimensional Correlation Analysis. *Phys. Rev. Lett.* **2010**, *105*, 266805.

(4) Makk, P.; Tomaszewski, D.; Martinek, J.; Balogh, Z.; Csonka, S.; Wawrzyniak, M.; Frei, M.; Venkataraman, L.; Halbritter, A. Correlation Analysis of Atomic and Single-Molecule Junction Conductance. *ACS Nano* **2012**, *6*, 3411-3423.